Supplementary Information B – Validation of Energy Arbitrage Model

The BESS and PHS behaviour are qualitatively described below. The scenarios depicted in the figures assume perfect price forecasting in order to demonstrate that the scheduling and charging modules are in close alignment. Under the assumption of imperfect price forecasting, the scheduling and charging module outputs would diverge due to differences between the forecast spot prices and actual dispatch prices.

Qualitative Description of BESS Behaviour

It can be seen in Figure S1 that the SOC for the following trading day (6 January 2019, SA1 region of NEM) is scheduled to increase while spot prices are low, then discharge when spot prices are high. Since perfect price forecasting was assumed, it is expected that the charging model outputs a SOC that maps onto the scheduled SOC almost exactly. Any discrepancies should be the result of errors created by linearising the power loss function or from ignoring the relationship between voltage efficiency and SOC in the scheduling constraints.

The day-ahead scheduled capacity for the BESS on the same trading day is plotted against the trading price in Figure S3. The dependence of scheduled capacity on spot price can be seen through the way in which the charging and discharging curves track the spot price curve reasonably closely, particularly during more extreme pricing events.

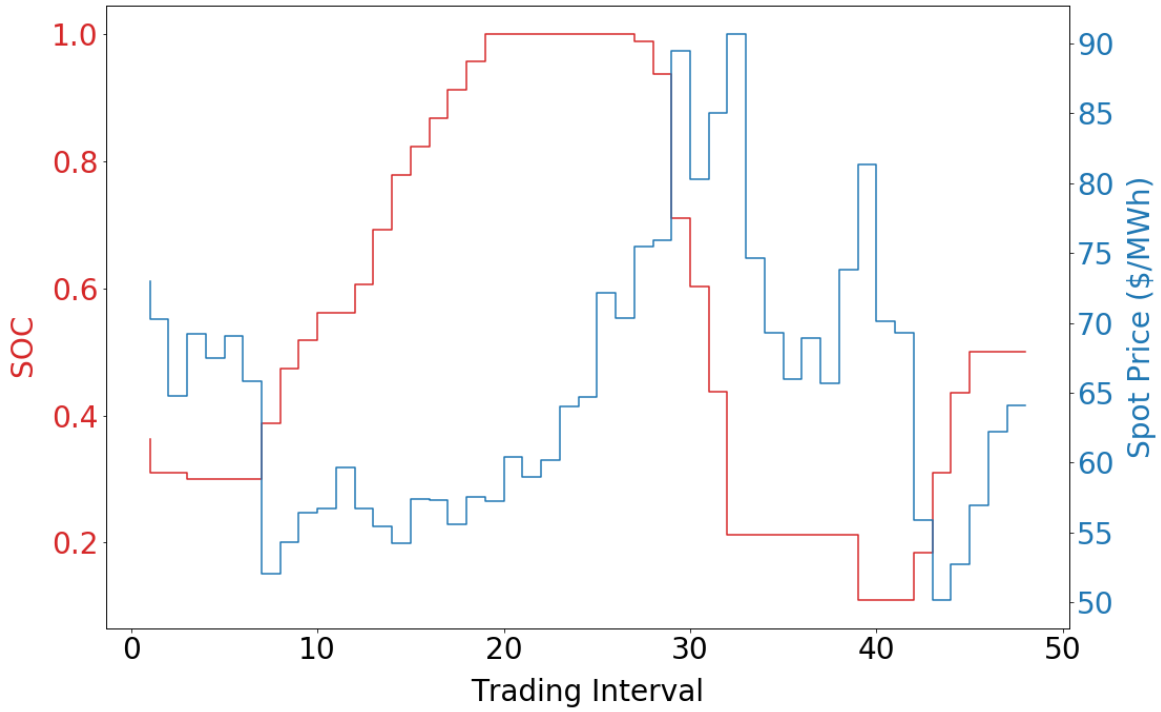


Figure S1. Day-ahead BESS Scheduled SOC with Perfect Price Forecasting (6 January 2019, SA1 Region).

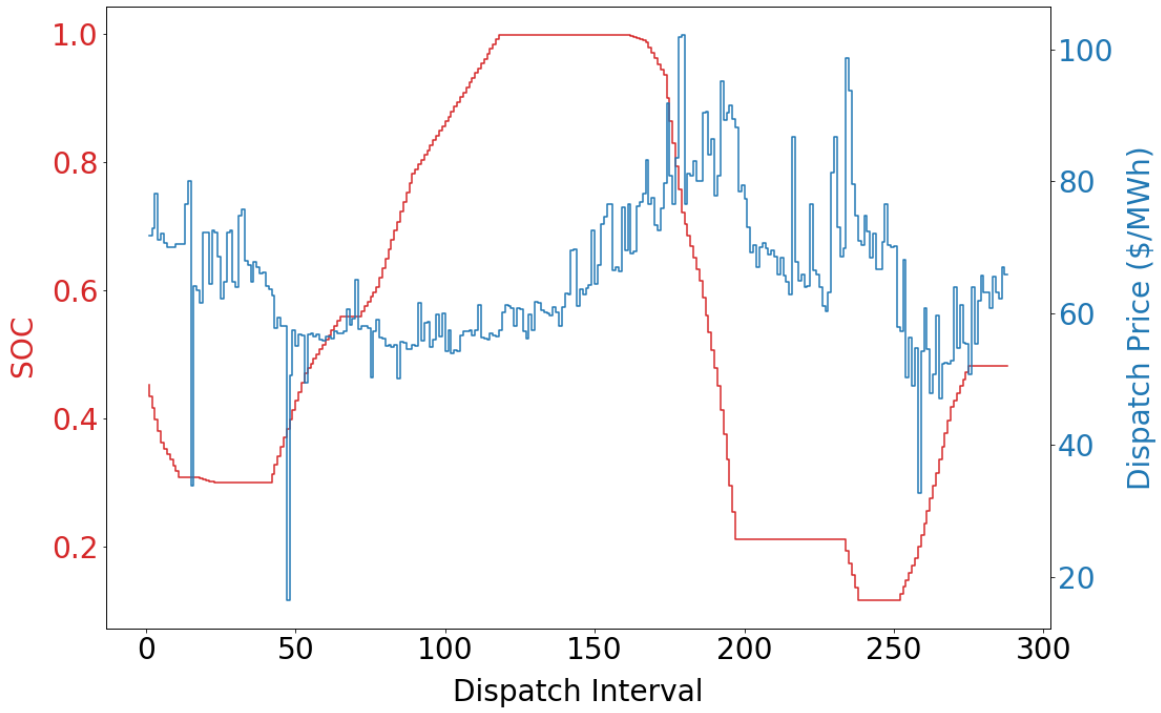


Figure S2. Actual BESS SOC on Trading Day (6 January 2019, SA1 Region).

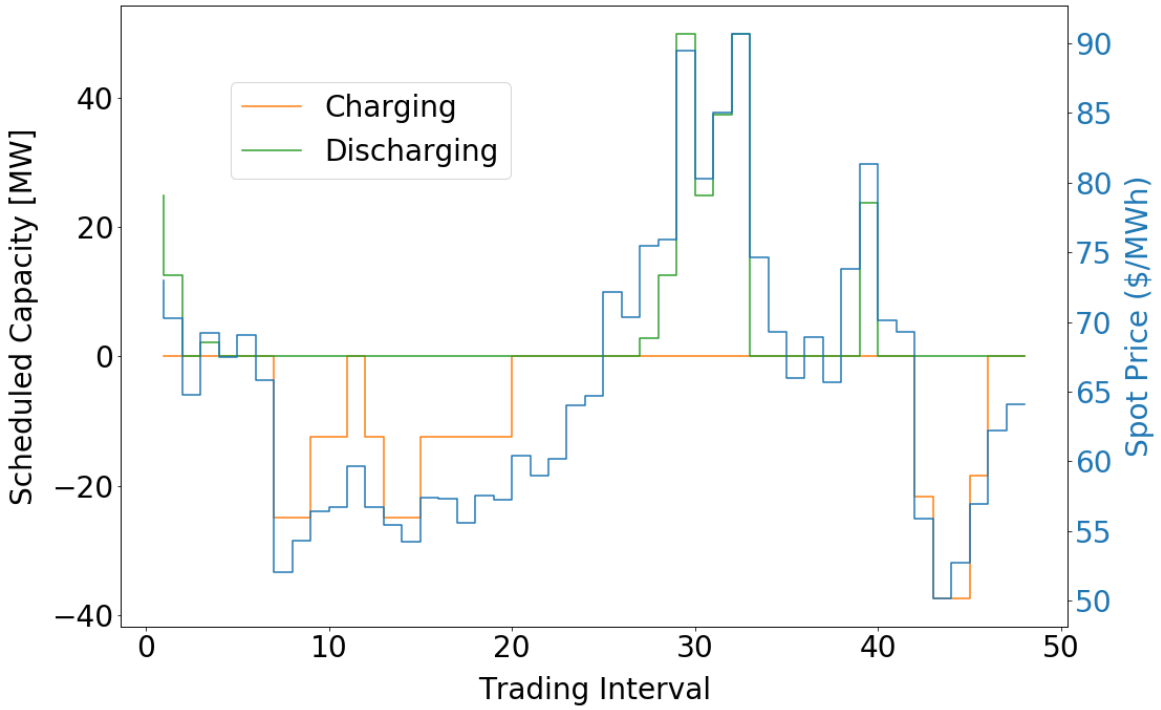


Figure S3. Day-ahead BESS Scheduled Capacity with Perfect Price Forecasting (6 January 2019, SA1 Region).

Qualitative Description of PHS Behaviour

The day-ahead scheduled SOC and the actual SOC for the validation scenario is plotted in Figure S4 and Figure S5 respectively. Notably, the SOC during charging drops below 46% and does not end the day at exactly 50%, unlike the scheduled SOC. The discrepancy is likely a result of the impact of using an effective head for scheduling, whilst the charging model is based upon non-linear functions using the actual net head during each dispatch interval. Changes in the net head could have a noticeable effect on the flow rate required to achieve scheduled powers, resulting in the upper reservoir being drained at a higher rate than predicted. Since the initial SOC at the start of each scheduling period equals the actual SOC at the end of the previous trading day, the impact of this error is not expected to propagate over time. Future improvements to the scheduling model could seek to develop the flow rate piece-wise linear functions to account for changes in net head, but there was a significant trade-off in optimisation time identified during testing of this solution.

An example of the scheduling behaviour of a PHS system under perfect and imperfect price forecasting conditions is provided in Figure S6 and Figure S7 respectively. The day-ahead scheduled capacity is also depicted for a system with two pumps and turbines that have the same capacity (Figure S8) as well as units with different capacities (Figure S9).

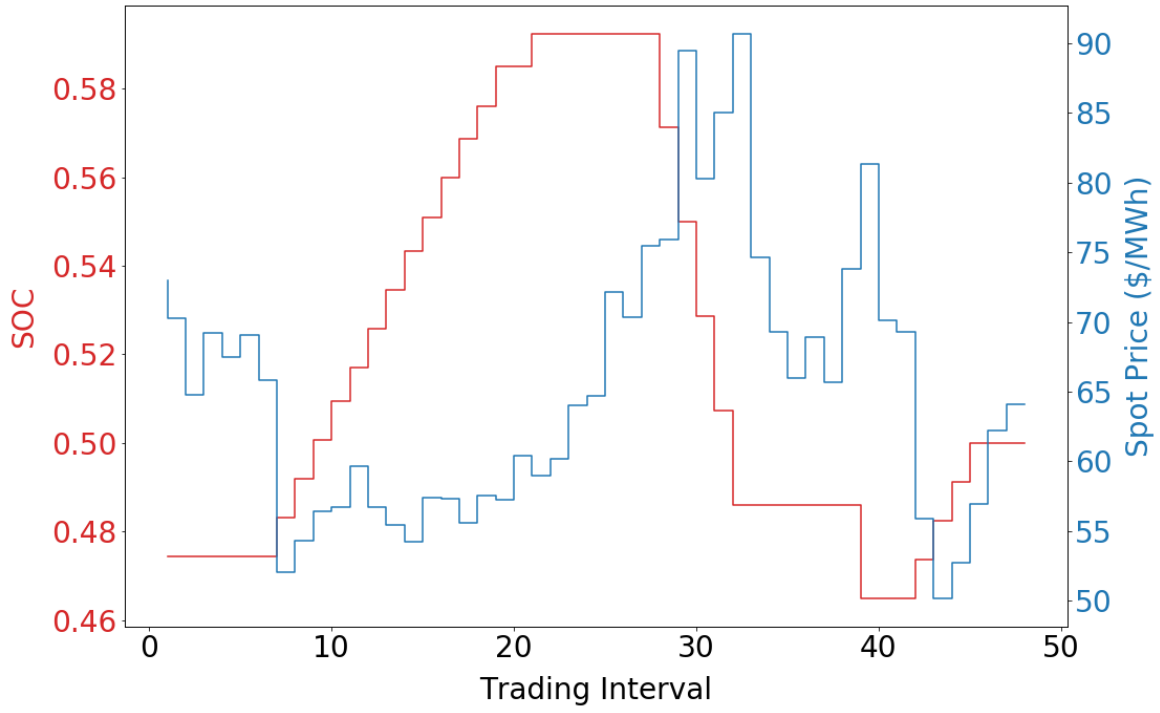


Figure S4. Day-ahead PHS Scheduled SOC with Perfect Price Forecasting (6 January 2019, SA1 Region).

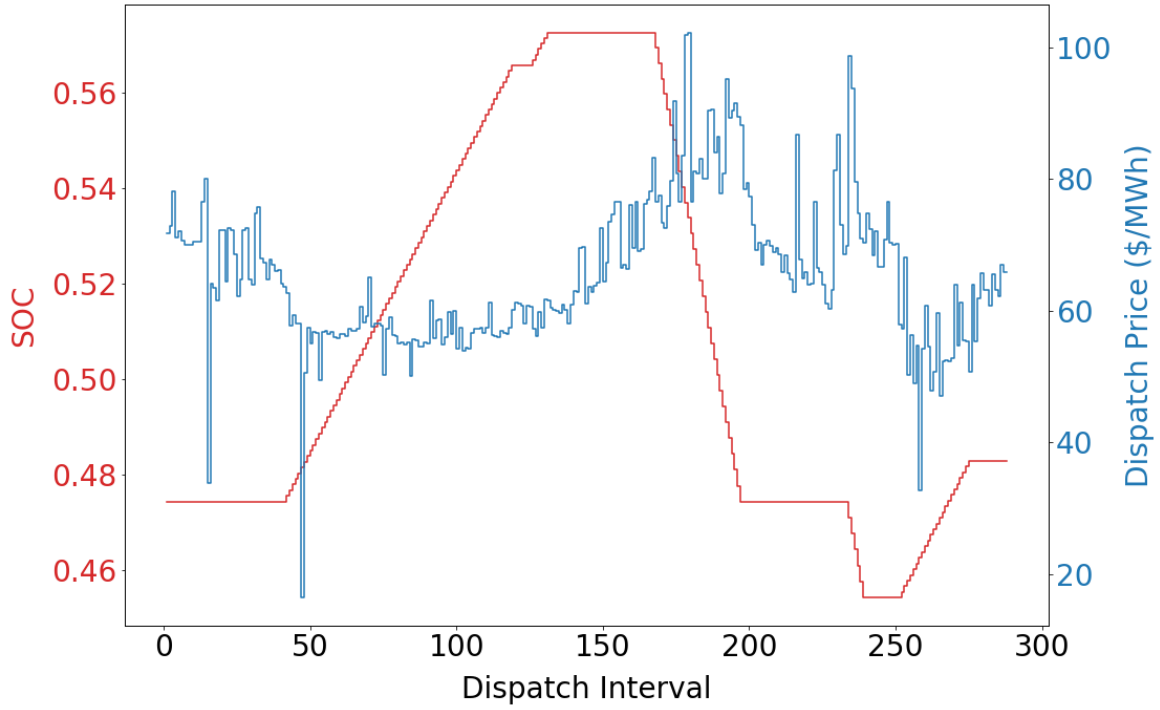


Figure S5. Actual PHS SOC on Trading Day (6 January 2019, SA1 Region).

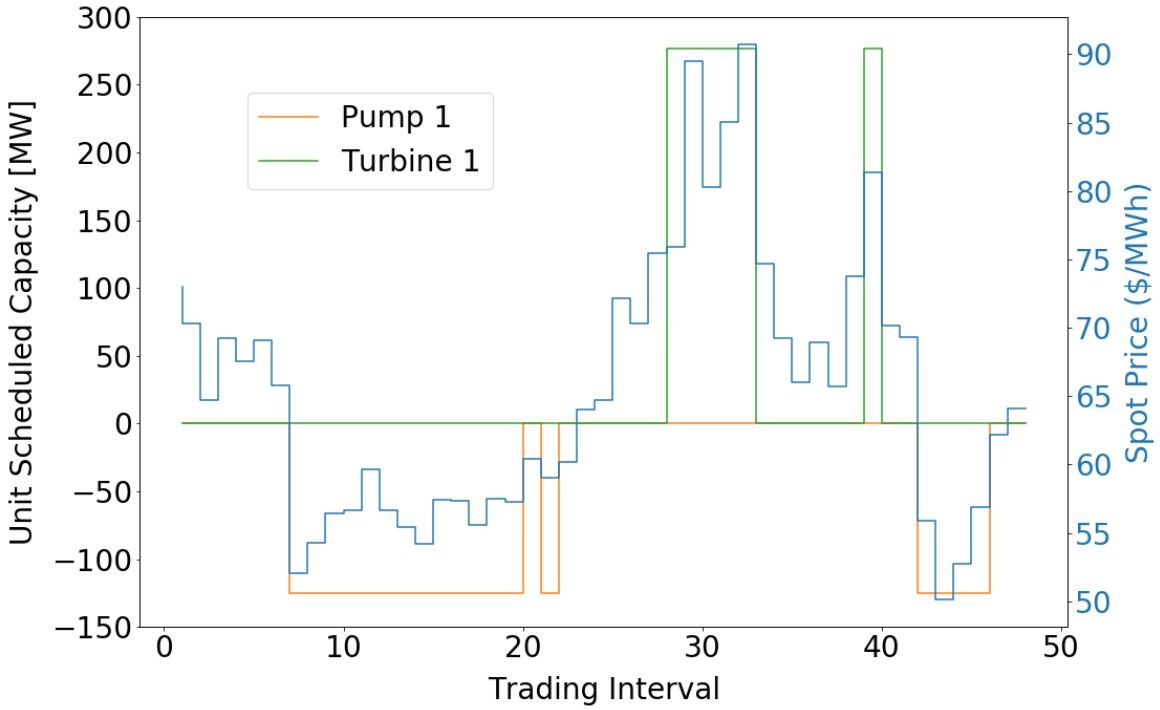


Figure S6. Day-ahead PHS Scheduled Capacity with Perfect Price Forecasting (6 January 2019, SA1 Region).

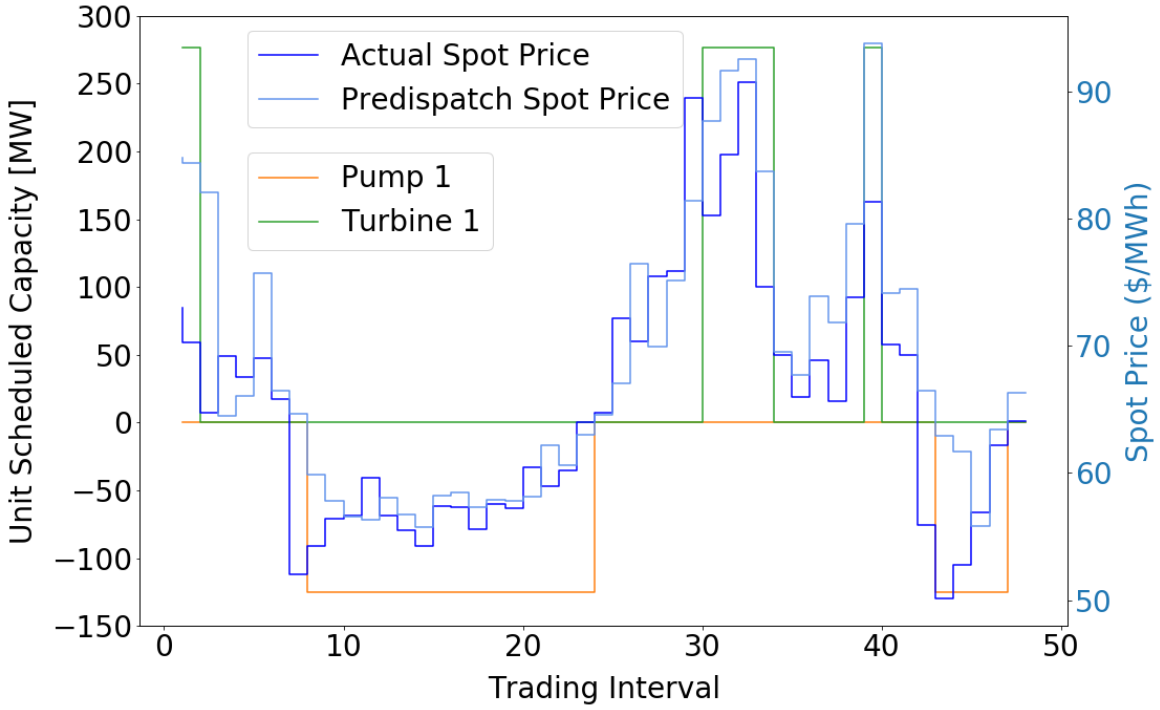


Figure S7. Day-ahead PHS Scheduled Capacity with Imperfect Price Forecasting (6 January 2019, SA1 Region).

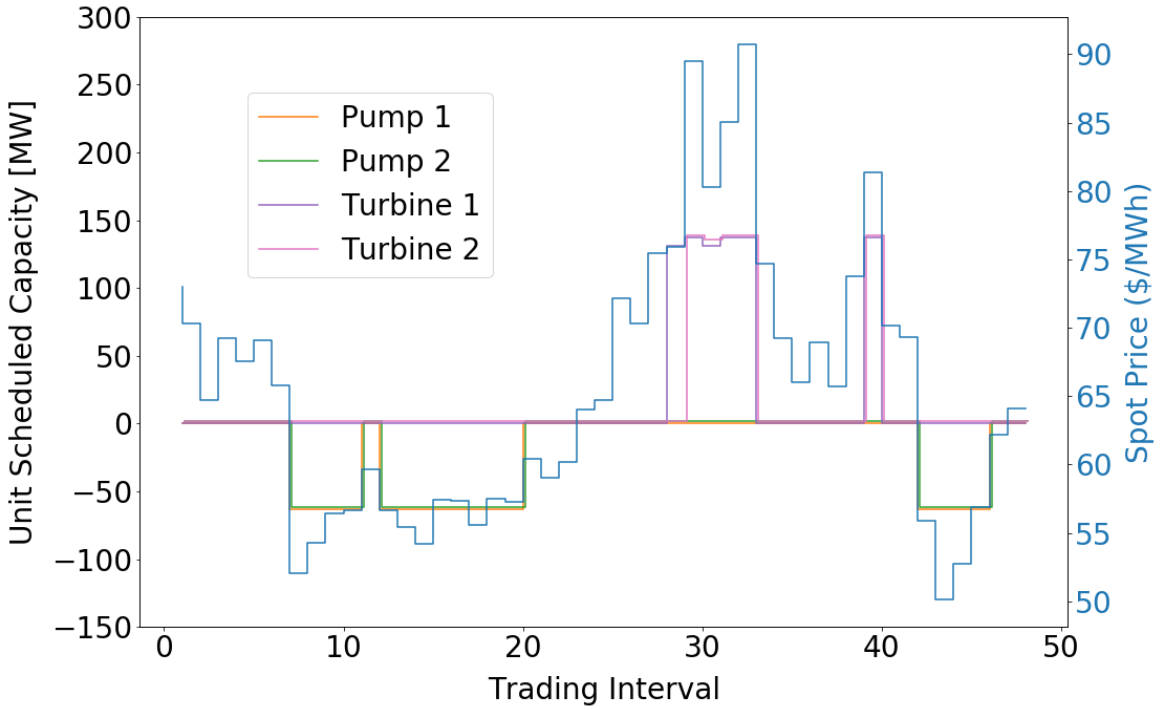


Figure S8. Day-ahead Symmetrical PHS Scheduled Capacity with Perfect Price Forecasting (6 January 2019, SA1 Region).

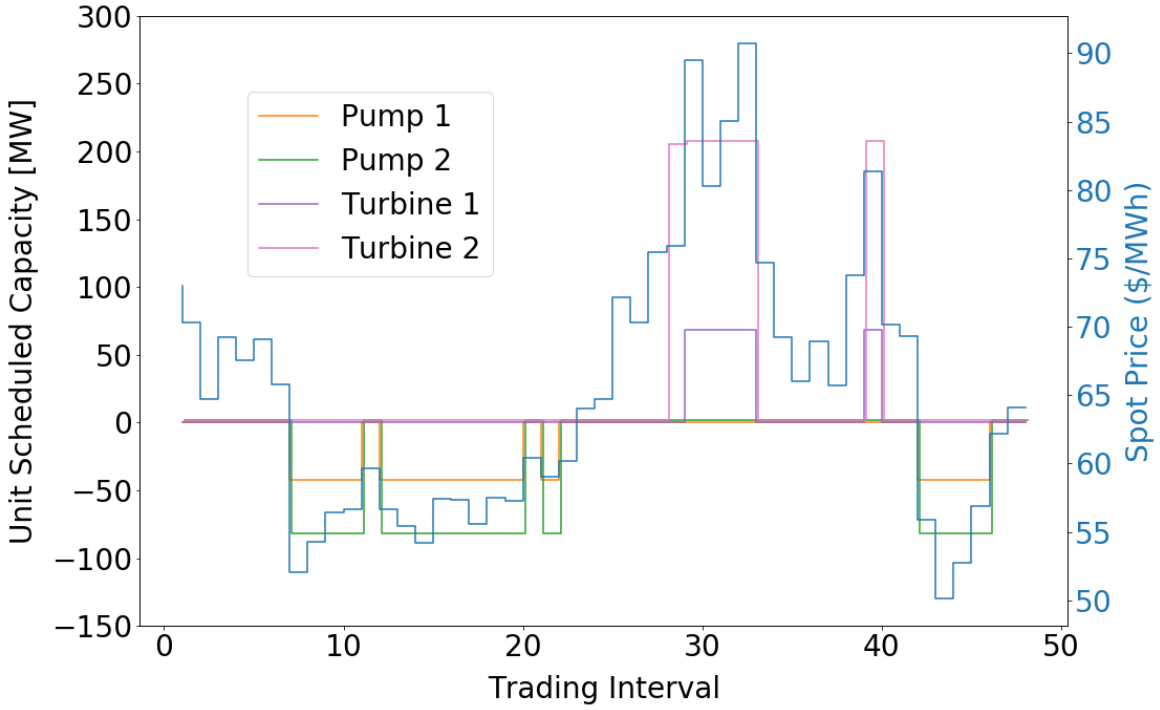


Figure S9. Day-ahead Asymmetrical PHS Scheduled Capacity with Perfect Price Forecasting (6 January 2019, SA1 Region).

BESS Key Parameters during Simulation

The open-circuit voltage of the BESS is described in Eq (33) – (35). These equations are repeated below for the convenience of the reader.

$$U_t^{\text{cell}} = \sum_{nn=1}^{n} \xi_n^{\text{cell}} \cdot \exp\left(-\left(\frac{SOC_t^{\text{test}} - \phi_n^{\text{cell}}}{\chi_n^{\text{cell}}}\right)^2\right) \tag{33}$$

$$U_{\text{nom}}^{\text{cell}} = \sum_{nn=1}^{n} \xi_n^{\text{cell}} \cdot \exp\left(-\left(\frac{0.5 - \phi_n^{\text{cell}}}{\chi_n^{\text{cell}}}\right)^2\right) \tag{34}$$

$$U_t^{\text{batt}} = U_t^{\text{cell}} N^{\text{series}} \tag{35}$$

The BESS open-circuit voltage as a function of SOC within the energy arbitrage model is depicted in Figure S10. This curve is based on the fitting parameters in Zhang, et al. [46]. For a comparison with experimental results, the reader is directed towards the paper by Zhang, et al.

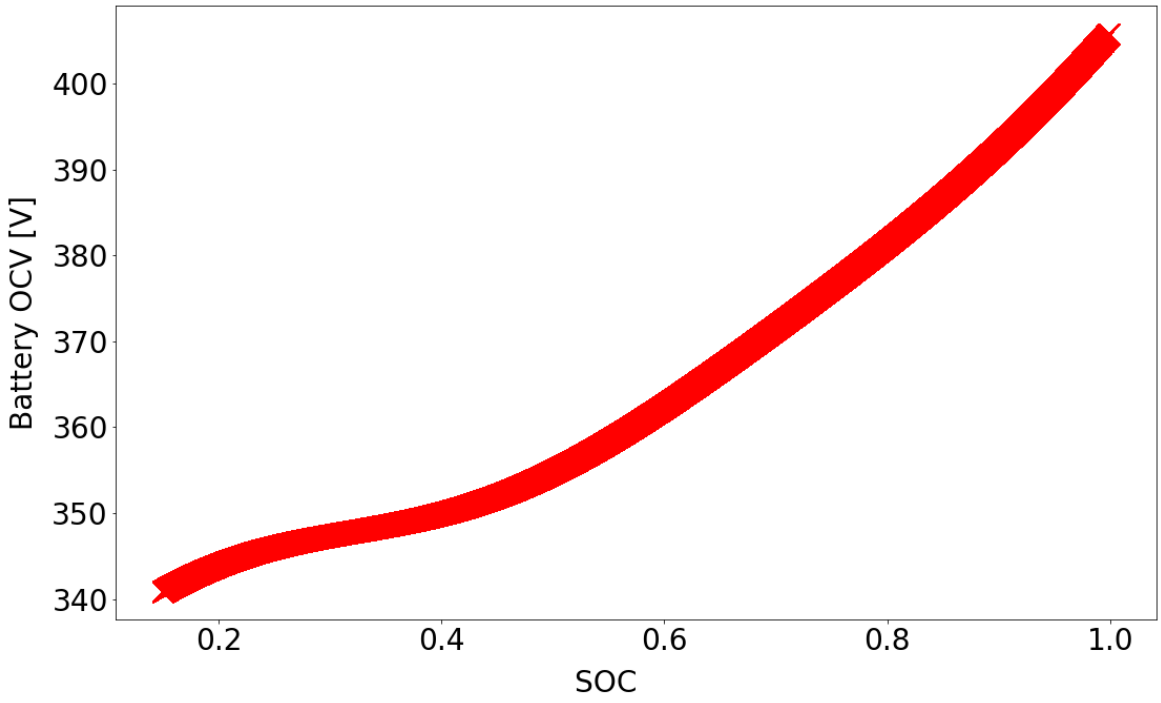


Figure S10. Battery Open-Circuit Voltage over First 80 Days of 2019.

The non-linear voltage efficiency of the battery, as determined within the charging module, is depicted in Figure S11. The equation for voltage efficiency, Eq (31), is repeated below. Note that open-circuit voltage is a function of SOC. Therefore, voltage efficiency is a function of dispatch power and SOC over relatively small time periods. Over long time periods, increases in the internal resistance of the battery due to aging will also impact the voltage efficiency.

$$\eta_t^{\text{volt}} = \frac{1}{2} + \sqrt{\frac{1}{4} - \frac{\left(P_{\text{gen},t}^{\text{disp}} + P_{\text{load},t}^{\text{disp}}\right)}{\eta^{\text{sys}} \cdot SOC_t^{\text{test}} \cdot CE^{\text{batt}}} \cdot \left(\frac{U_{\text{nom}}^{\text{batt}}}{U_t^{\text{batt}}}\right)^2 \cdot \frac{ir_t^{\text{cell}} \cdot CE^{\text{cell}}}{U_{\text{nom}}^{\text{cell}}}} \quad (31)$$

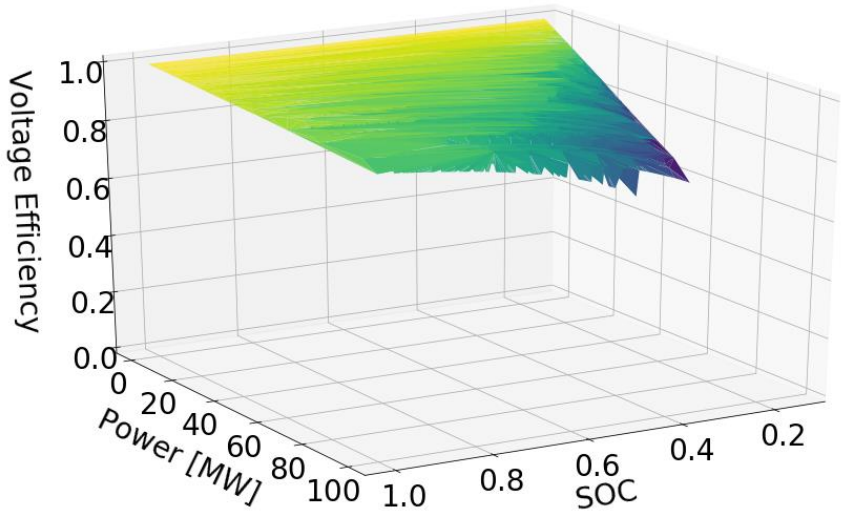


Figure S11. Battery Voltage Efficiency over First 80 Days of 2019.

The degradation in battery energy capacity, represented by the state-of-health of the system, is demonstrated in Figure S12. While the empirical degradation model provides a reasonable description of battery degradation over the long term, the state-of-health may not be accurately compared between nearby dispatch intervals. A first principles degradation model would provide a better description of short-term degradation.

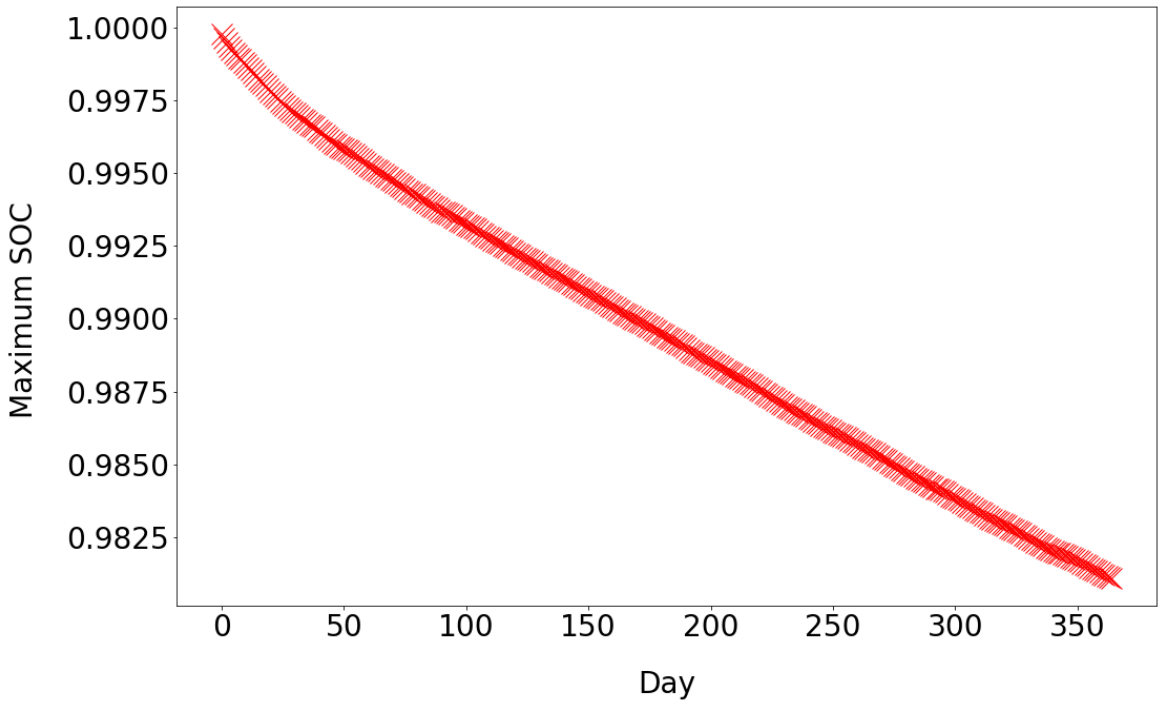


Figure S12. Modelled BESS State-of-Health at the End of Each Day in 2019.

PHS Key Parameters during Simulation

The net head of the PHS, as described by Eq (8) and (9), for a single trading day is depicted in Figure S13. Net head is given as a function of SOC since the upper and lower reservoir water levels are both a function of SOC. At a higher SOC, the system has a higher net head since the upper water level is higher relative to the lower water level.

$$H_t^{\mathrm{p}} = h^{\mathrm{r}} + h_t^{\mathrm{uwl}} + h^{\mathrm{lr}} - h_t^{\mathrm{lwl}} + H_t^{\mathrm{pl}} \tag{8}$$

$$H_t^{t} = h^{\mathrm{r}} + h_t^{\mathrm{uwl}} + h^{\mathrm{lr}} - h_t^{\mathrm{lwl}} - H_t^{\mathrm{tl}} \tag{9}$$

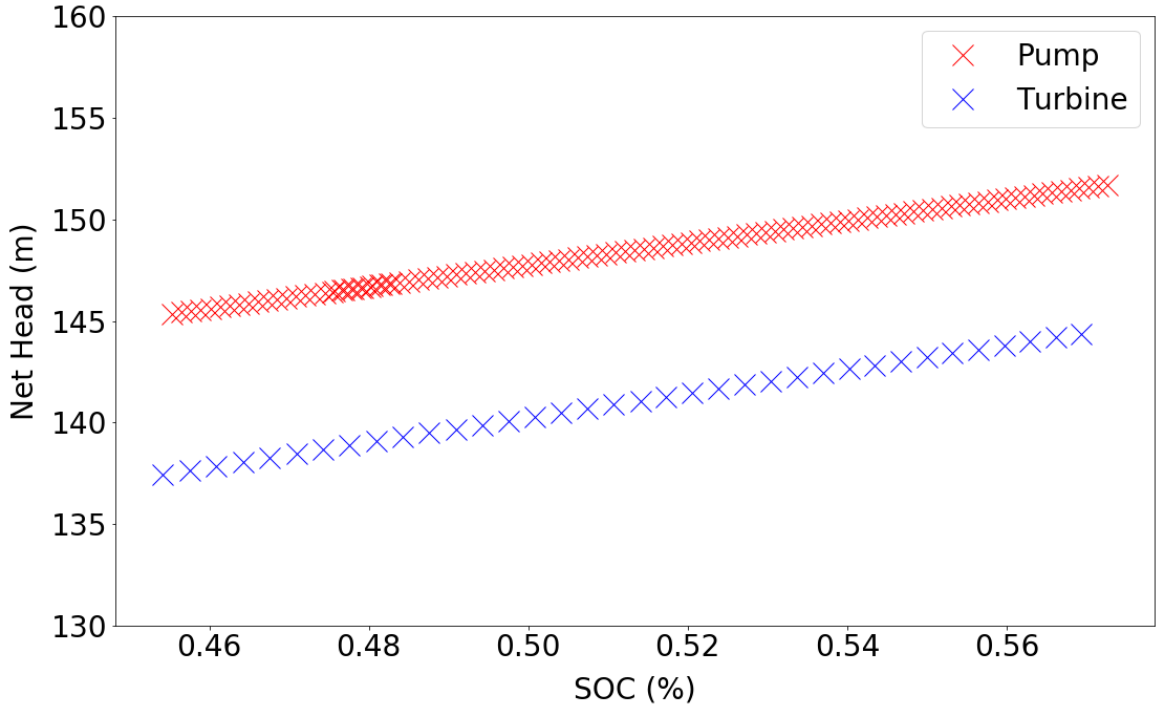


Figure S13. Net Heads on Trading Day (6 January 2019, SA1 Region).

Pump and turbine head losses impact the net head due to energy losses within the penstock. At a high level, they are described by Eq (10) – (11) and (16) – (17). Since the penstock characteristics remain unchanged over the course of the simulation for one PHS, the head loss can be described as a function of water flow rate through the pump or turbine (Figure S14). Flow rate for the pump is relatively constrained since it is assumed to only operate at rated conditions, while the turbine is allowed to operate over at all flow rates outside the cavitation conditions. Turbine efficiency is also a function of flow rate. The turbine efficiency calculated for intervals within the simulation is provided in Figure S15.

$$H_t^{\mathrm{pl}} = \frac{K_t^{\mathrm{p}} \cdot \left(WV_t^{\mathrm{p}}\right)^2}{2g} \tag{10}$$

$$WV_t^{\mathrm{p}} = \frac{\Sigma_g \, Q_{t,g}^{\mathrm{p}}}{0.25 \cdot \pi \cdot (PD^{\mathrm{p}})^2} \tag{11}$$

$$H_t^{\mathrm{tl}} = \frac{K_t^{\mathrm{t}} \cdot \left(WV_t^{\mathrm{t}}\right)^2}{2g} \tag{16}$$

$$WV_t^{\mathrm{t}} = \frac{\Sigma_h \, Q_{t,h}^{\mathrm{t}}}{0.25 \cdot \pi \cdot (PD^{\mathrm{t}})^2} \tag{17}$$

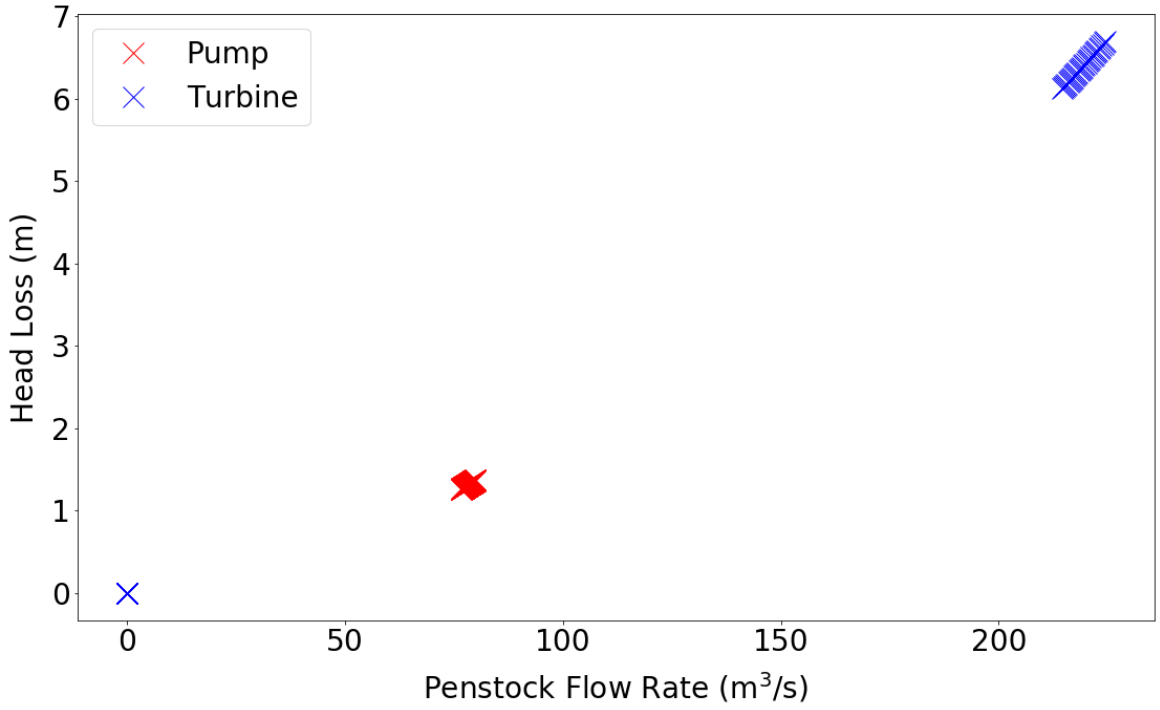


Figure S14. Head Losses on Trading Day (6 January 2019, SA1 Region).

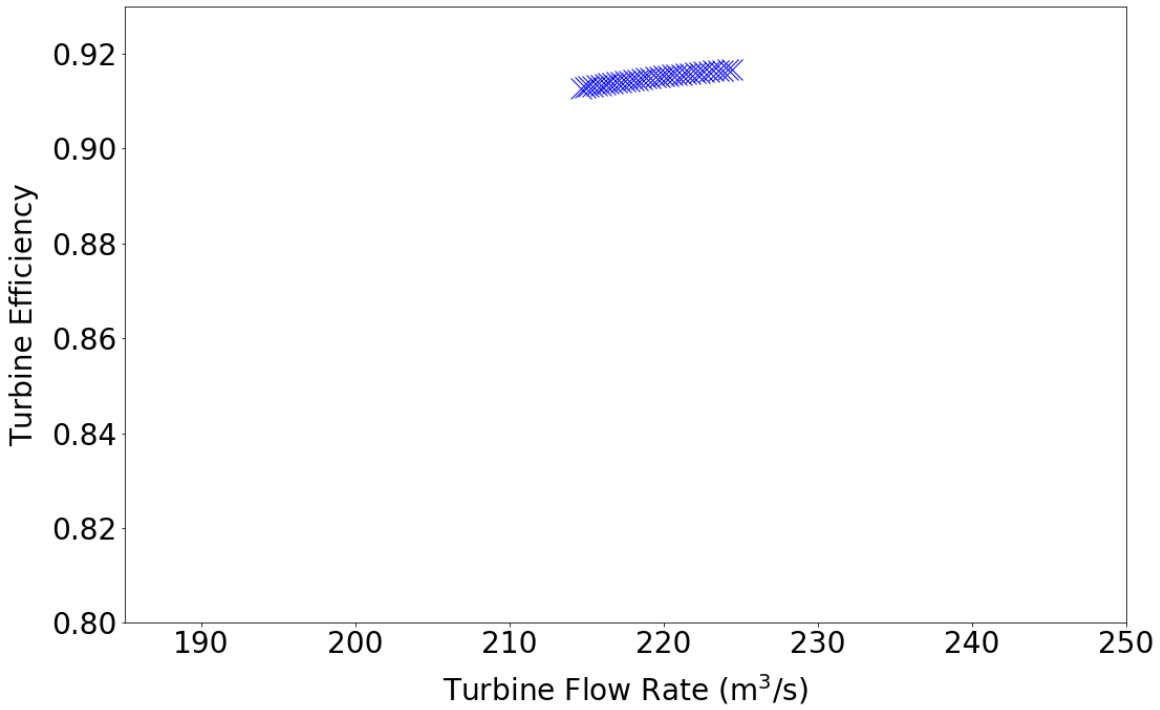


Figure S15. Turbine Efficiency on Trading Day (6 January 2019, SA1 Region).

Arbitrage Model Validation Against Expected Values

Table 1. Model Validation Tests.

Scenario	Key Assumptions	Test	Expected Value	Model Value	Comments
Degradation-free BESS	Perfect forecasting, no risk hedging, no degradation	Mean difference between scheduled SOC and corresponding SOC during charging	0 %	1.03 %	Model value greater than expected value due to approximations inherent to linearising the power loss function and ignoring influence of variable SOC on voltage efficiency within scheduling module.
		Scheduled capacity relative to spot price Kendall Tau-b for one day	>> 0 , ≤ 1	0.82	Tested using 6 January 2019 in SA1. Would expect 1 for a single cycle. Less than 1 due to more than one cycle per day, with a difference in median spot price for the cycles.
		Scheduled capacity relative to spot price Kendall Tau-b over many days	> 0, ≤ 1	0.3587	Tested using first 80 days of 2019 in SA1. Less than Tau-b for one day due to changes in median spot price over many cycles and overlap between cycles.
		Battery open-circuit voltage range	> 150 V, < 1000 V	> 340.8 V, < 406.0 V	The SMA Sunny Tripower inverters were used to define the expected voltage range [68]. Based on the assumed cell characteristics and configuration, the model output a voltage range within the expected bounds.

		Voltage efficiency range	> 85.1%, < 100%	> 67.0%, < 100%	Based on all dispatch intervals in 1 year. Scheduling attempts to keep total efficiency (voltage and system efficiency) above 80%. It is based upon average SOC during a particular trading interval. During charging, actual SOC in a dispatch interval may be as low as 15%, so high powers scheduled for these trading intervals may result in voltage efficiency < 85.1% for the first few dispatch intervals. The number of dispatch intervals that experience this low voltage efficiency is small over the entire simulation.
BESS charging model with degradation	Perfect forecasting, no risk hedging, capacity and efficiency fading	Lifetime of battery (i.e. time until SOH = 80%)	~ 10 – 15 years	16.3 years	AEMO assumes a technical life of 10 years for new BESS projects [58]. Tesla also offers a 10-year no defect and energy retention warranty for its Powerwall, as well as a 15-year no defect and energy retention warranty for its Powerpack and Megapack Li-ion storage systems [69]. The degradation rate in the arbitrage model defines a system on the upper end of the

					expected lifetime, though the degradation rate will vary based upon the region and simulation year. Note that the case studies in this project assume BESS lifetime of 10 years to reduce simulation time. This is not expected to impact the results of the case studies since we are not looking to calculate the actual return on investment, only look at levelized cost of storage trends and modelling methods.
		Calendar aging capacity loss vs number of dispatch intervals Kendall Tau-b over many days	~1	0.9985	Tested using first 80 days of 2019 in SA1. Slightly less than 1 since calendar aging uses average SOC of battery. Therefore, degradation appropriate for long-term analysis, but not short-term.
		Cycle aging capacity loss vs dispatch interval charging energy throughput Kendall Tau-b over many days	~1	0.9998	Tested using first 80 days of 2019 in SA1. Slightly less than 1 since cycle aging uses average cell current. Therefore, degradation appropriate for long-term analysis, but not short-term.
		Average daily internal resistance of	~1	1.0000	Tested using first 80 days of 2019 in SA1. Since internal

		cells vs number of days			resistance uses average SOC, degradation appropriate for long-term analysis, but not short term.
Single pump/turbine PHS with no mode change time	Perfect forecasting, no risk hedging, no transient behaviour, single pump and turbine	Scheduled capacity relative to spot price Kendall Tau-b for one day	≥ 0.67, ≤ 1	0.8120	Since pump capacity equals half of the turbine capacity, must spend approximately twice as much time charging as discharging. Ties between charging capacities and idle capacities (0 MW) move the Tau-b closer to 1.
		Scheduled capacity relative to spot price Kendall Tau-b over many days	> 0, ≤ 1	0.4675	Tested using first 80 days of 2019 in SA1. Less than Tau-b for one day due to changes in median spot price over many cycles and overlap between cycles.
		Mean difference between scheduled SOC and corresponding SOC during charging	0 %	0.2%	Mean difference likely primarily caused by assumption of effective head during scheduling. Could reduce scheduling error by further partitioning flow rate loss linear function along the head axis, but was noted to greatly increase computation time. Model values determined from all

					dispatch intervals in 2019.
		Net head range	> 9 m, < 400 m	> 128.6 m, < 156.6 m	Expected value based upon rule of thumb for Francis turbine selection [70]. Model values determined from all dispatch intervals in 2019.
		Turbine efficiency range during discharging	> 91.6 %	> 90.2 %	Limits of cavitation development within the operating range of Francis turbine used to define efficiency range [71]. Model values determined from all dispatch intervals in 2019. Likely minor cavitation. Future iterations of the model could constrain turbine flow rate even more. Minimum efficiency is appropriate for the analysis in this project.
		Turbine flow rate range during discharging	> 214 m/s^3 < 236 m/s^3	> 200 m/s^3 < 240 m/s^3	Limits of cavitation development within the operating range of Francis turbine used to define flow rate range [71]. Model values determined from all dispatch intervals in 2019. Likely minor cavitation conditions. Future iterations of the model could constrain turbine flow rate even more.
Single pump/turbine	Perfect forecasting,	Difference in AADP relative	> –1 %, < 1 %	– 0.61 %	Expect negligible change if ignoring

PHS with mode change time	no risk hedging, transient behaviour, single pump and turbine	to no transient time			transient behaviour during scheduling is to be justified.
		Difference in RADP relative to no transient time	> –1 %, < 1 %	– 0.01 %	Expect negligible change if ignoring transient behaviour during scheduling is to be justified.
Single pump/turbine PHS with imperfect price forecasting	Imperfect forecasting, no risk hedging, transient behaviour, single pump and turbine	Scheduled capacity relative to spot price Kendall Tau-b for one day	>> 0, < Tau-b for perfect forecasting	0.7033	0.7033 < 0.8120 as expected. Expect imperfectly forecast price to correlate with actual spot price, but discrepancies between these sets of price sets reduces the dependence of scheduled capacity on actual spot price
		Scheduled capacity relative to spot price Kendall Tau-b over many days	> 0, < Tau-b for perfect forecasting	0.4121	0.4121 < 0.4675 as expected. Expect imperfectly forecast price to correlate with actual spot price, but discrepancies between these sets of price sets reduces the dependence of scheduled capacity on actual spot price